Maternal diet disrupts the placenta-brain axis in a sex-specific manner

Alexis M Ceasrine[1], Benjamin A Devlin[1], Jessica L. Bolton[2], Lauren A. Green[1], Young Chan Jo[1], Carolyn Huynh[1], Bailey Patrick[1], Kamryn Washington[1], Cristina L. Sanchez[4], Faith Joo[1], A. Brayan Campos-Salazar[3], Elana R. Lockshin[3], Cynthia Kuhn[4], Susan K. Murphy[5], Leigh Ann Simmons[6], Staci D. Bilbo*[1,3,7]

[1]Department of Psychology and Neuroscience, Duke University, Durham, NC, USA
[2]Neuroscience Institute, Georgia State University, Atlanta, GA, USA
[3]Department of Neurobiology, Duke University Medical Center, Durham, NC, USA
[4]Department of Pharmacology and Cancer Biology, Duke University Medical Center, Durham, NC, USA
[5]Department of Obstetrics and Gynecology, Duke University Medical Center, Durham, NC, USA
[6]Department of Human Ecology, Perinatal Origins of Disparities Center, University of California, Davis, California, USA
[7]Lurie Center for Autism, Massachusetts General Hospital, Boston, MA

SUMMARY: High maternal weight is associated with a number of detrimental outcomes in offspring, including increased susceptibility to neurological disorders such as anxiety, depression, and communicative disorders (e.g. autism spectrum disorders)[1–8]. Despite widespread acknowledgement of sex-biases in the prevalence, incidence, and age of onset of these disorders, few studies have investigated potential sex-biased mechanisms underlying disorder susceptibility. Here, we use a mouse model to demonstrate how maternal high-fat diet, one contributor to overweight, causes endotoxin accumulation in fetal tissue, and subsequent perinatal inflammation influences sex-specific behavioral outcomes in offspring. In male high-fat diet offspring, increased macrophage toll like receptor 4 signaling results in excess phagocytosis of serotonin neurons in the developing dorsal raphe nucleus, decreasing serotonin bioavailability in the fetal and adult brain. Bulk sequencing from a large cohort of matched first trimester human fetal brain, placenta, and maternal decidua samples reveals sex-specific transcriptome-wide changes in placenta and brain tissue in response to maternal triglyceride accumulation (a proxy for dietary fat content). Further, we find that fetal brain serotonin levels decrease as maternal dietary fat intake increases in males only. These findings uncover a microglia-dependent

34 mechanism through which maternal diet may impact offspring susceptibility for
35 neuropsychiatric disorder development in a sex-specific manner.

36 **MAIN:** In the United States, more than 50% of women are overweight or obese when they
37 become pregnant[9], and elevated maternal weight is associated with adverse outcomes
38 in offspring, particularly increased incidence of neuropsychiatric disorders such as
39 anxiety, and depression[1–8]. Diets high in saturated fats are one major contributor to
40 overweight and obesity[10]. Thus, we sought to dissect the contribution of a maternal high-
41 fat diet (mHFD) to offspring risk for neuropsychiatric disorder development.

42 Rodent and non-human primate models have implicated perinatal high-fat diet in
43 the establishment of offspring anxiety[11–13]. Decades of research into anxiety and
44 depression have strongly linked disruptions in the serotonin (5-HT) system as causal to
45 neuropsychiatric diseases such as anxiety and depression. Although women
46 disproportionately bear the burden of these disorders[14,15], little has been done to
47 investigate the contribution of 5-HT to anxiety/depression on the basis of sex.
48 Understanding the developmental mechanisms through which sex contributes to
49 neuropsychiatric disorder development, susceptibility, and severity in response to
50 environmental exposures such as diet is of utmost importance when considering clinical
51 implications such as treatment efficacy.

52 **<u>Maternal high-fat diet imparts sex-specific offspring behavioral outcomes</u>**

53 To interrogate the contribution of maternal dietary fat content to offspring
54 neurological development, female wild-type (*C57BL/6J*) mice were placed on either a
55 high-fat (45% kcal from fat; HFD) or low-fat (10% kcal from fat, sucrose matched; LFD)
56 diet at approximately 4 weeks of age (juvenile) for six weeks prior to mating (Fig 1a).

Starting females on HFD during the juvenile period best mimics trends observed in fat consumption in human populations – juveniles tend to get more calories from high-fat foods, and their eating patterns as adults tend to mimic their adolescent eating patterns[16–20]. HFD females gained significantly more weight than LFD females before pregnancy and their weight remained elevated throughout gestation (Extended Data Fig 1a-b). No significant differences were observed in litter size, composition, or maternal care (during either the light or dark phase; Extended Data Fig 1c-e). Both male and female maternal high-fat diet (mHFD) offspring weighed significantly more than maternal low-fat diet (mLFD) offspring throughout life, though placental weight at embryonic day 14.5 (e14.5)

Fig 1. Maternal high-fat diet imparts sex-specific offspring behavioral outcomes.

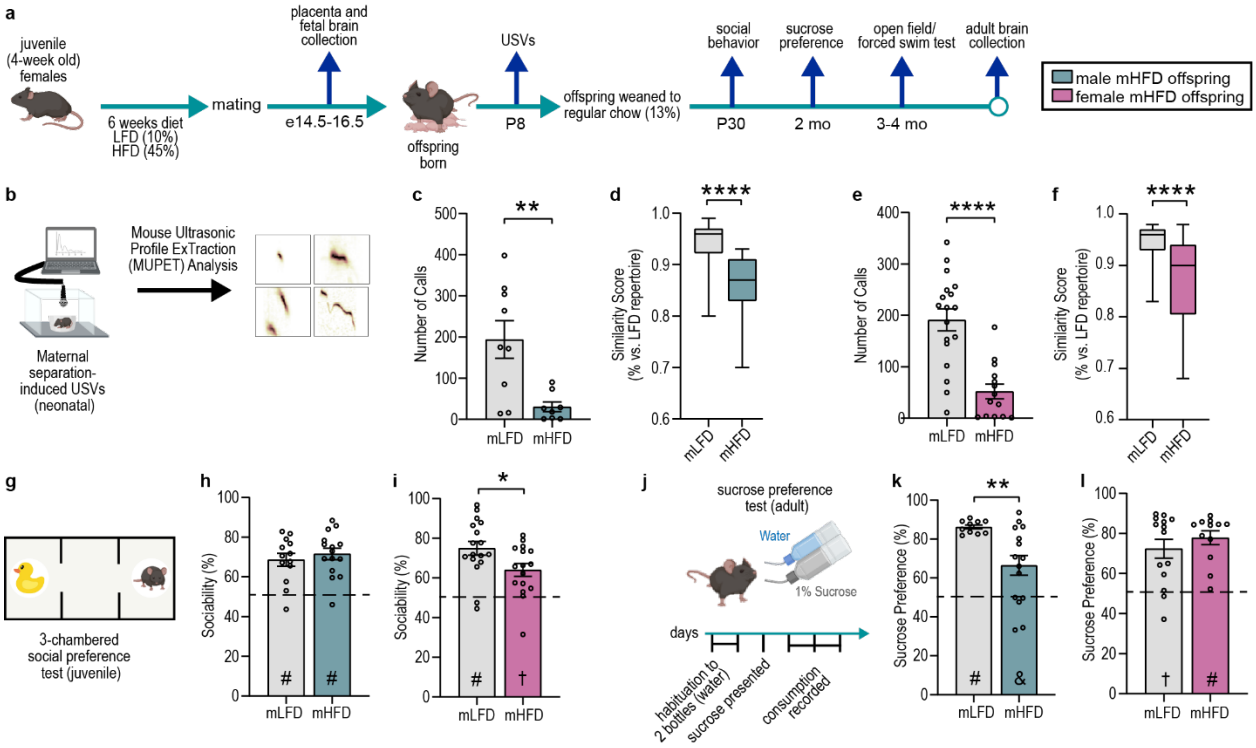

a, Schematic of maternal low-fat and high-fat diet paradigm (10% and 45% represent %kcal from fat in diet). **b,** Schematic of neonatal maternal separation-induced ultrasonic vocalization (USV) recording and analysis. **c-f,** mHFD decreases neonatal USV number and syllable repertoire similarity in male and female offspring (n=9 mLFD, 8 mHFD male offspring; 18 mLFD, 14 mHFD female offspring from 5 mLFD and 4 mHFD litters). **g,** Schematic of 3-chambered social preference test. **h,** Male mLFD and mHFD offspring display a strong social preference (n=13 mLFD, 15 mHFD male offspring from 5 mLFD and 6 mHFD litters). **i,** Female mHFD offspring have a reduced social preference versus mLFD offspring (n=17 mLFD, 16 mHFD female offspring from 6 mLFD and 6 mHFD litters). **j,** Schematic of sucrose preference test. **k,** Male mHFD offspring display a decreased preference for sucrose versus mLFD offspring (n=10 mLFD, 15 mHFD male offspring from 5 mLFD and 5 mHFD litters). **l,** Female mLFD and mHFD offspring display a strong sucrose preference (n=14 mLFD, 12 mHFD female offspring from 5 mLFD and 5 mHFD litters). Data are mean ± s.e.m.; asterisk denoted p-values are derived from unpaired two-tailed t-tests (**c, e, i, k**) or paired two-tailed t-tests (**d, f**). other p-values (# p<0.0001, † p<0.001, & p<0.01) are derived from one-sample t-tests assessing difference from chance (50%) (**h, i, k, l**).

66 was not affected by mHFD (Extended Data Fig 1f-g). Offspring behavior was assessed
67 at neonatal, juvenile, and adult time-points (Fig 1a).

68 Neonatal maternal separation-induced ultrasonic vocalizations (USVs) provide a
69 readout of early communicative behaviors in mice, and peak at postnatal day 8 in
70 *C57BL/6J* mice[21,22]. USV analyses (Fig 1b) revealed a significant decrease in the number
71 of USVs emitted, total call time, mean call length, and mean syllable number along with
72 a significant increase in inter-syllable interval in both male (Fig 1c, Extended Data Fig 2a-
73 e) and female (Fig 1e, Extended Data Fig 2g-k) mHFD offspring compared to same sex
74 mLFD offspring. Female, but not male, mHFD offspring USVs had a higher mean
75 frequency (kHz) compared to mLFD offspring (Extended Data Fig 2d, j). To rule out a
76 potential shift in USV peak in mHFD offspring, we quantified USVs at P7 and P10 in
77 addition to P8, but mHFD offspring called less across the assessed neonatal window
78 (Extended Data Fig 2f, l). In-depth characterization of overall USV composition
79 (integrating alterations in frequency (kHz), energy (dB), and syllable complexity [e.g.
80 number of syllables, frequency of calls]) using Mouse Ultrasonic Profile ExTraction
81 (MUPET[23]) revealed a significant decrease in USV similarity (an integrated measure of
82 call parameters, see methods for more detail) between mLFD and mHFD male (Fig 1d)
83 and female (Fig 1f) offspring. While less is known about what USV complexity may
84 represent in neonates, adult USVs are context-dependent, and specific USV parameters
85 such as frequency (kHz) are known to vary in response to a stressful environment[24]. To
86 parse out whether the USV changes were reflective of an overall lack of social
87 engagement in mHFD offspring, we assessed juvenile sociability using a 3-chamber
88 social preference test (Fig 1g). Male mHFD offspring showed no change in sociability,

time investigating the social stimulus, or time in the social chamber when compared to controls (Fig 1h; Extended Data Fig 2m). Female mHFD offspring had a significantly decreased sociability score, driven by female mHFD offspring spending significantly less time investigating the social stimulus as compared to controls (Fig 1i; Extended Data Fig 2o). Interestingly, USV emission (number of calls) at P8 significantly positively correlated with social behavior in females only (r^2=0.39, p=0.006 for females, r^2=0.004, p=0.78 for males), suggesting that decreased USVs may predict impaired social behavior in females, but not in males. In a complementary social novelty preference (SNP) assay, male mHFD showed no change in SNP, time investigating the novel social stimulus, or time in the novel social chamber compared to mLFD controls (Extended Data Fig 2n). Female mHFD offspring had a significantly decreased SNP score, driven by female mHFD offspring spending significantly less time investigating the novel social stimulus and less time in the novel social stimulus chamber compared to mLFD controls (Extended Data Fig 2p). To better understand the behavioral changes affecting male mHFD offspring, we determined average sucrose preference over a 3-day free-choice test (Fig 1j). Mice normally display a strong preference for sucrose, and diminished sucrose preference is one measure of anhedonia, or lack of reward/pleasure. Average sucrose preference was significantly decreased in male, but not female, mHFD offspring (Fig 1k-l). Neither male nor female mHFD offspring showed a change in total liquid consumption (water + sucrose) over the 3-day testing period (Extended Data Fig 3a,f), and there was no correlation between body weight and sucrose preference within either mLFD or mHFD groups. We additionally assessed mobility behavior in a forced swim test (FST; Extended Data Fig 3b). Male mHFD offspring spent significantly less time immobile, moved significantly further, and

with a higher velocity than mLFD offspring (Extended Data Fig 3c-e). No changes were observed in FST behavior in female mHFD offspring compared to female mLFD offspring (Extended Data Fig 3g-i). Lastly, neither male nor female mHFD offspring had any changes in general activity or anxiety-like behavior in an open field test (OFT; Extended Data Fig 3j-r). This suggests that the social deficits observed in females are not due to impaired motor skills or an anxiety-like phenotype, and that the increased velocity and distance moved by males in the FST are not due to general hyperactivity. In sum, despite some similar behavioral phenotypes in USVs in early life, by adolescence and into adulthood the behavior patterns diverge based on sex, with mHFD female offspring showing social deficits, and mHFD male offspring showing diminished non-social reward behavior and increased activity in the FST.

mHFD decreases 5-HT in male offspring and increasing 5-HT levels is sufficient to prevent behavioral phenotypes

We observed altered neonatal USVs, anhedonia, and increased activity during the FST in male mHFD offspring. These behaviors are associated with diminished brain 5-HT (5-HT) in mice[25–29]. Previous research has demonstrated that brain 5-HT levels during discrete windows of development are dependent on placental 5-HT synthesis[30]. The placenta is a temporary organ that develops during early gestation and surrounds the fetus to both restrict and facilitate macromolecule and nutrient transport. Further, the placenta acts as a critical interface between the maternal environment and the developing fetal brain and responds to maternal diet/environment in a fetal sex-specific manner[31–33]. However, a potential role for fetal sex in placental 5-HT production is unknown. Assessment of 5-HT levels in mLFD and mHFD placenta and fetal forebrain revealed a

Fig 2. mHFD decreases 5-HT in male offspring and increasing 5-HT levels is sufficient to prevent behavioral phenotypes

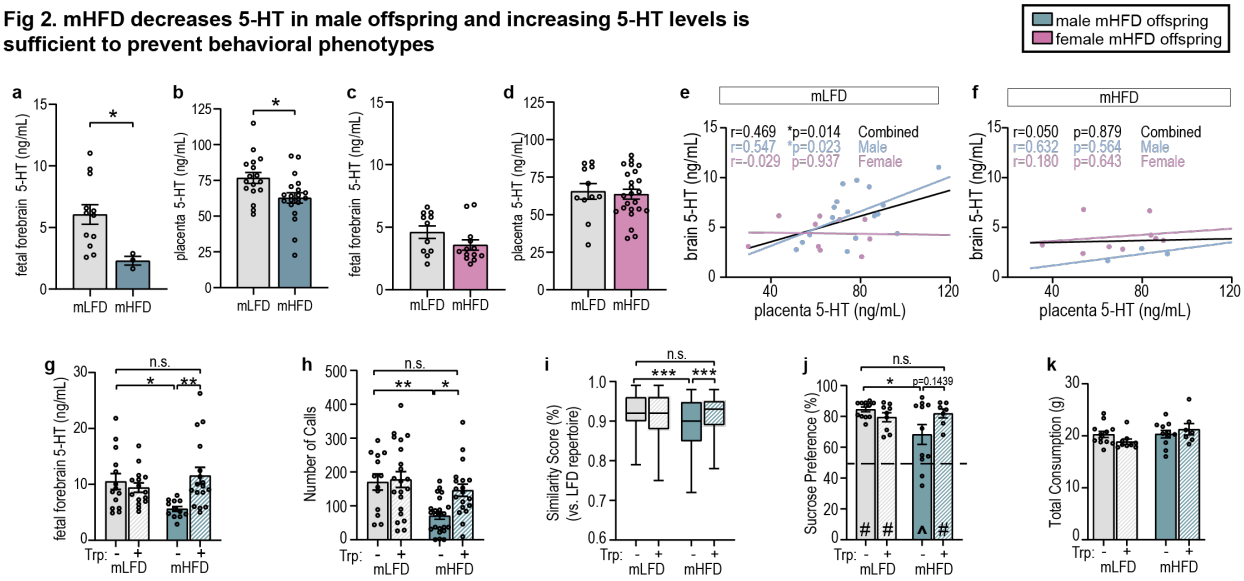

a, Male mHFD offspring have decreased fetal forebrain serotonin (n=12 mLFD, 3 mHFD male offspring from 3 mLFD and 3 mHFD litters). **b,** Male mHFD offspring have decreased placenta serotonin (n=18 mLFD, 20 mHFD offspring from 4 mLFD and 6 mHFD litters). **c-d,** mHFD does not impact fetal serotonin levels in female offspring (forebrain: n=11 mLFD, 13 mHFD from 3 mLFD and 3 mHFD litters; placenta: n=11 mLFD, 24 mHFD female offspring from 4 mLFD and 6 mHFD litters) **e-f,** Fetal serotonin levels are significantly correlated between brain and placenta in mLFD males only (n=17 male, 10 female mLFD offspring from 4 mLFD litters; 3 male, 9 female mHFD offspring from 3 mHFD litters). **g,** Maternal dietary tryptophan enrichment increases serotonin levels in mHFD fetal male forebrain (n=14 mLFD, 15 mLFD+Trp, 12 mHFD, 17 mHFD+Trp offspring from 5 mLFD, 5 mLFD+Trp, 3 mHFD, and 5 mHFD+Trp litters) **h-i,** Maternal dietary tryptophan enrichment rescues mHFD-induced decrease in USV number and syllable repertoire similarity (n= 13 mLFD, 21 mLFD+Trp, 23 mHFD, 19 mHFD+Trp offspring from 5 mLFD, 7 mLFD+Trp, 8 mHFD, and 7 mHFD+Trp litters). **j-k,** Maternal dietary tryptophan enrichment rescues sucrose preference in mHFD male offspring and does not affect total consumption (n= 12 mLFD, 9 mLFD+Trp, 11 mHFD, 7 mHFD+Trp male offspring from 6 mLFD, 5 mLFD+Trp, 5 mHFD, and 6 mHFD+Trp litters). Data are mean ± s.e.m. asterisk denoted p-values are derived from unpaired two-tailed t-tests (**a, b**), Pearson's correlation (**e, f**), or two-way ANOVA (fat content x tryptophan content; **g, h, i, j**). other p-values (# p<0.0001, ^p<0.05) are derived from one-sample t-tests assessing difference from chance (50%) (**j**). n.s. not significant.

male-specific decrease in tissue 5-HT in mHFD offspring (Fig 2a-d, also see Extended Data Fig 4d-g). Circulating maternal 5-HT levels were not changed by HFD, suggesting that this regulation is within fetal tissue (Extended Data Fig 4a). In agreement with previous studies demonstrating that placental 5-HT correlates with fetal brain 5-HT[30], we observed a significant positive correlation between placental and fetal forebrain 5-HT in mLFD offspring (Fig 2e, see also Extended Data Fig 5f). Interestingly, the correlation was exclusively driven by male 5-HT levels, but mHFD disrupted the correlation between placental and brain 5-HT levels in males, potentially a floor effect due to low 5-HT levels (Fig 2f, see also Extended Data Fig 5g).

Quantitative real-time PCR (qPCR) showed a decrease in both the 5-HT synthesis enzyme tryptophan hydroxylase 2 (*Tph2*) and the 5-HT transporter (*5HTT*) in male mHFD

146 placenta (Extended Data Fig 4b-c). To better understand the dynamics of placental 5-HT
147 in response to mHFD, we additionally quantified levels of 5-HT, the 5-HT precursor
148 tryptophan, and the 5-HT metabolite 5-hydroxyindoleacetic acid (5-HIAA), in the placenta
149 using high-performance liquid chromatography (HPLC; Extended Data Fig 4d-g and
150 ExtendedDataFig4_RawData_Stats). In agreement with decreased *Tph2* levels, 5-HT
151 synthesis (ratio of 5-HT to tryptophan) was significantly decreased in male, but not
152 female, mHFD offspring placenta (Extended Data Fig 4d, f). We did not observe any
153 changes in the expression of the alternate 5-HT synthesis enzyme tryptophan
154 hydroxylase 1 (*Tph1*), monoamine oxidase A (*MAOA*), an enzyme responsible for the
155 oxidative deamination of neurotransmitters, including 5-HT, or the rate-limiting enzyme
156 indoleamine 2,3-dioxygenase (*Ido1*) that promotes the degradation of tryptophan through
157 the kynurenine pathway in male placentas (Extended Data Fig 4b). In line with this, we
158 also did not observe any changes in the protein levels of quinolinic acid, and kynurenic
159 acid levels were undetectable in e14.5 brain and placental tissue, suggesting that
160 tryptophan is not being diverted into the kynurenine pathway in mHFD offspring
161 (Extended Data Fig4h-i). Comparing the ratio of 5-HIAA to 5-HT (5-HT turnover) revealed
162 a modest but significant increase in 5-HT turnover in male mHFD offspring placenta,
163 suggesting that in addition to diminished 5-HT synthesis, increasing turnover may
164 contribute to total decreased placental 5-HT levels in male mHFD offspring (Extended
165 Data Fig 4d). In the fetal forebrain, we did not see changes in 5-HT synthesis or turnover,
166 but we did see a decrease in tryptophan in both male and female mHFD offspring
167 (Extended Data Fig 4e, g). Lastly, *MAOA* expression was significantly decreased in
168 female mHFD placenta, suggesting that an alternate neurotransmitter may be affected in

169 female mHFD offspring, and that the placenta may play a critical role as a source for brain
170 neurotransmitters other than 5-HT (Extended Data Fig 4c).

171 To determine if increasing 5-HT in male mHFD offspring could rescue the mHFD-
172 induced behavioral outcomes, we sought to rescue 5-HT by supplementing the maternal
173 low- and high-fat diets with tryptophan. Tryptophan is the precursor to 5-HT, and placental
174 5-HT levels are largely dependent on maternal tryptophan levels[30,32]. Tryptophan
175 supplementation (+Trp; provided in LFD or HFD chow for the same duration as in Fig 1a)
176 did not affect maternal weight gain, litter composition (i.e., size and sex ratio), or offspring
177 weights (Extended Data Fig 5a-d).

178 Maternal tryptophan supplementation increased placental 5-HT levels in male
179 mLFD offspring (Extended Data Fig 5e) in support of previous literature demonstrating
180 that placental 5-HT levels are dependent on maternal tryptophan levels. In male mHFD
181 offspring, tryptophan supplementation was unable to substantially increase placental 5-
182 HT levels (Extended Data Fig 5e). Conversely, maternal tryptophan supplementation did
183 increase fetal forebrain 5-HT levels in male mHFD, but not mLFD offspring (Fig 2g).
184 Further, Pearson correlation analyses demonstrated that maternal tryptophan enrichment
185 disrupted the significant positive correlation between brain and placental 5-HT levels in
186 male mLFD offspring (Extended Data Fig 5f). No significant correlation was detected in
187 mHFD (in agreement with our previous finding) or mHFD+Trp offspring (Extended Data
188 Fig 5g). This suggests that in mHFD+Trp offspring, the fetal brain produces 5-HT
189 independently of the placenta. Together these data demonstrate that in males, placental
190 5-HT levels are dependent on maternal tryptophan levels and can be disrupted by
191 maternal diet, but fetal forebrain 5-HT levels are not solely dependent on placental 5-HT

192 levels. Further, mHFD led to decreased 5-HT levels in adult male midbrain – where the
193 majority of 5-HT neuronal cell bodies reside – levels that were also rescued by maternal
194 tryptophan enrichment (Extended Data Fig 5h).

195 To determine if mHFD-induced behavioral deficits in male offspring were rescued
196 by maternal tryptophan supplementation, we assessed USVs and sucrose preference in
197 male mLFD and mHFD offspring. Tryptophan supplementation did not impact USV or
198 sucrose preference behavior in male mLFD offspring (Fig 2h-k, Extended Data Fig5 i-m).
199 However, in mHFD offspring, maternal tryptophan supplementation fully rescued the
200 decreased USV call number and similarity, as well as the increased inter-syllable interval
201 (Fig 2h-i, Extended Data Fig 5k), partially rescued the deficits seen in total USV call time,
202 mean call length, and mean syllable number (Extended Data Fig5 i-m), as well as the
203 diminished sucrose preference (Fig 2j-k). In all cases, mHFD+Trp offspring behavior was
204 indistinguishable from that of mLFD or mLFD+Trp offspring. Of note, maternal tryptophan
205 supplementation rescued male mHFD offspring USV phenotypes despite the observation
206 that male mHFD+Trp offspring still weigh more than mLFD and mLFD+Trp offspring (see
207 Extended Data Fig 5c), suggesting that changes in offspring weight is not driving the USV
208 phenotypes. Further, maternal tryptophan supplementation did not alter male offspring
209 social behavior or open field behavior (Extended Data Fig 5n-u).

210 Although we did not expect to see a rescue of behavioral phenotypes in female
211 mHFD+Trp offspring because mHFD did not impact 5-HT levels in females, we assessed
212 midbrain 5-HT and behavior outcomes. Adult female offspring midbrain 5-HT levels were
213 unaffected by mHFD or tryptophan supplementation (Extended Data Fig 6a). Maternal
214 tryptophan enrichment did not rescue female mHFD offspring USV behavior, but

interestingly did decrease USV call similarity and call length in mLFD offspring (Extended Data Fig 6b-h). Maternal tryptophan supplementation also increased USV frequency (kHz) in female offspring regardless of maternal dietary fat content (Extended Data Fig 6g). This suggests that despite similar neonatal behavioral outcomes in male and female mHFD offspring, the mechanisms driving USV behavior in males and females may be distinct. Interestingly, maternal tryptophan enrichment increased sucrose preference in female offspring regardless of maternal dietary fat intake (Extended Data Fig 6i). Maternal tryptophan enrichment did not rescue female mHFD social behavior deficits (Extended Data Fig 6j-m). In sum, these data demonstrate 1) a developmental role for 5-HT in males that is perturbed by maternal high-fat diet, and 2) that maternal tryptophan enrichment is sufficient to rescue mHFD-induced brain 5-HT deficiency and associated 5-HT-dependent behaviors in males.

mHFD induces Tlr4-dependent inflammation driving offspring behavior changes

Maternal HFD creates an environment of chronic inflammation that affects the developing fetus as well as the placenta[34]. Growing literature has demonstrated complex relationships between inflammation and 5-HT[35–37], and we hypothesized that the mHFD-induced inflammatory environment is translated to the fetus, and responsible for decreased 5-HT in male mHFD offspring. At e14.5, we observed increased macrophage (F4/80+ cells located on the fetal side of the placenta) density in male and female mHFD placenta (Extended Data Fig 7a), as well as increased Iba1 and CD68 immunoreactivity (labeling microglia and phagosomes, respectively) in both male and female fetal dorsal raphe nuclei (DRN), where the majority of serotonergic cell bodies reside (Fig 3a). Microglia influence central circuits in numerous ways, such as by pruning excess

238 synapses or phagocytosing excess or dying progenitor cells[38–41]. Interestingly, qPCR for
239 genes important for phagocytosis from isolated midbrain microglia at e14.5 did not reveal
240 any significant changes in gene expression, although the levels of some genes were near
241 or below the limit of detection (see Methods, Extended Data Fig 7b). Given the increased
242 immunoreactivity seen by immunohistochemistry (IHC), we further investigated potential
243 interactions between microglia and the developing central 5-HT system by 3D
244 reconstructing microglia from e14.5 DRN. IMARIS reconstructions revealed that 5-HT
245 signal comprised a higher percentage of phagosomes (CD68) in male mHFD microglia
246 *versus* mLFD (Fig 3b), demonstrating that microglial phagocytosis of serotonergic
247 neurons is increased in males in the context of mHFD, leading to decreased central 5-HT
248 bioavailability. Postnatal microglia express the 5-HT receptor 5HT2B[42] and decrease their
249 phagocytic capacity in response to 5-HT[43]. Further, mice lacking microglial 5HT2B display
250 prolonged neuroinflammation in response to lipopolysaccharide (LPS), a classic agonist
251 of macrophage toll-like receptor signaling[44]. Thus, we sought to investigate potential
252 feedback between 5-HT levels and microglial phagocytosis of 5-HT neurons. Microglial
253 5-HT phagocytosis was rescued in mHFD+Trp offspring, in parallel with 5-HT levels (Fig
254 3b; see Figure 2g), suggesting that in the context of mHFD, enrichment of 5-HT levels is
255 sufficient to prevent further aberrant microglia phagocytosis. Consistent with our
256 observations that mHFD does not decrease 5-HT levels in females, we did not see
257 increased 5-HT signal within phagosomes in mHFD female microglia (Extended Data Fig
258 7c). Interestingly, there was a significant increase in 5-HT signal within phagosomes in
259 reconstructed microglia from mHFD+Trp female microglia (Extended Data Fig 7c),
260 possibly contributing to the trend towards lower midbrain 5-HT we observed in the adult

261 female mHFD+Trp offspring (see Extended Data Fig 6a). This trend parallels the open
262 field behavior, with mHFD+Trp female offspring showing increased activity in the open
263 field test (see Extended Data Fig 6n-o), suggesting that fetal microglial interactions with
264 5-HT neurons may dictate different behaviors in males and females.

265 The presence of 5-HT receptors on placental macrophages, or the potential
266 influence of 5-HT on placental macrophages is unknown, although recent studies have
267 demonstrated the presence of functional 5-HT transporters in placental tissue[45,46]. Thus,
268 we sought to investigate crosstalk between placental 5-HT and placental macrophage
269 density as well as fetal brain 5-HT and microglial activity. Maternal tryptophan
270 supplementation did not significantly influence placental macrophage density in either
271 mLFD or mHFD male or female offspring (Extended Data Fig 7d). Considering our finding
272 that male mLFD+Trp offspring have increased placental 5-HT (see Extended Data Fig
273 5e), this suggests that placental macrophage density is not significantly influenced by 5-
274 HT.

275 To further investigate the potential pro-inflammatory pathways leading to
276 increased placental macrophage and fetal brain microglia density, we assessed a panel
277 of pro-inflammatory markers with qPCR (Extended Data Fig 7e). This revealed a specific
278 increase in Toll-like receptor 4 (Tlr4) in both male and female mHFD placenta (Extended
279 Data Fig 7e). Tlr4 is a pattern recognition receptor known to initiate pro-inflammatory
280 signaling cascades in response to infectious pathogens (e.g. bacterial, viral), and whose

281 expression is increased in response to saturated fats/obesity[47–50]. Isolated fetal microglia

282 and placental macrophages from obese dams have exaggerated cytokine production in

283 response to lipopolysaccharide (LPS), a classic Tlr4 agonist[33].

284 To determine if increased *Tlr4* signaling in macrophages was causal to decreased

285 5-HT and 5-HT-dependent behaviors in males, or to behavioral changes in females, we

Fig 3. mHFD induces Tlr4-dependent inflammation driving offspring behavior changes

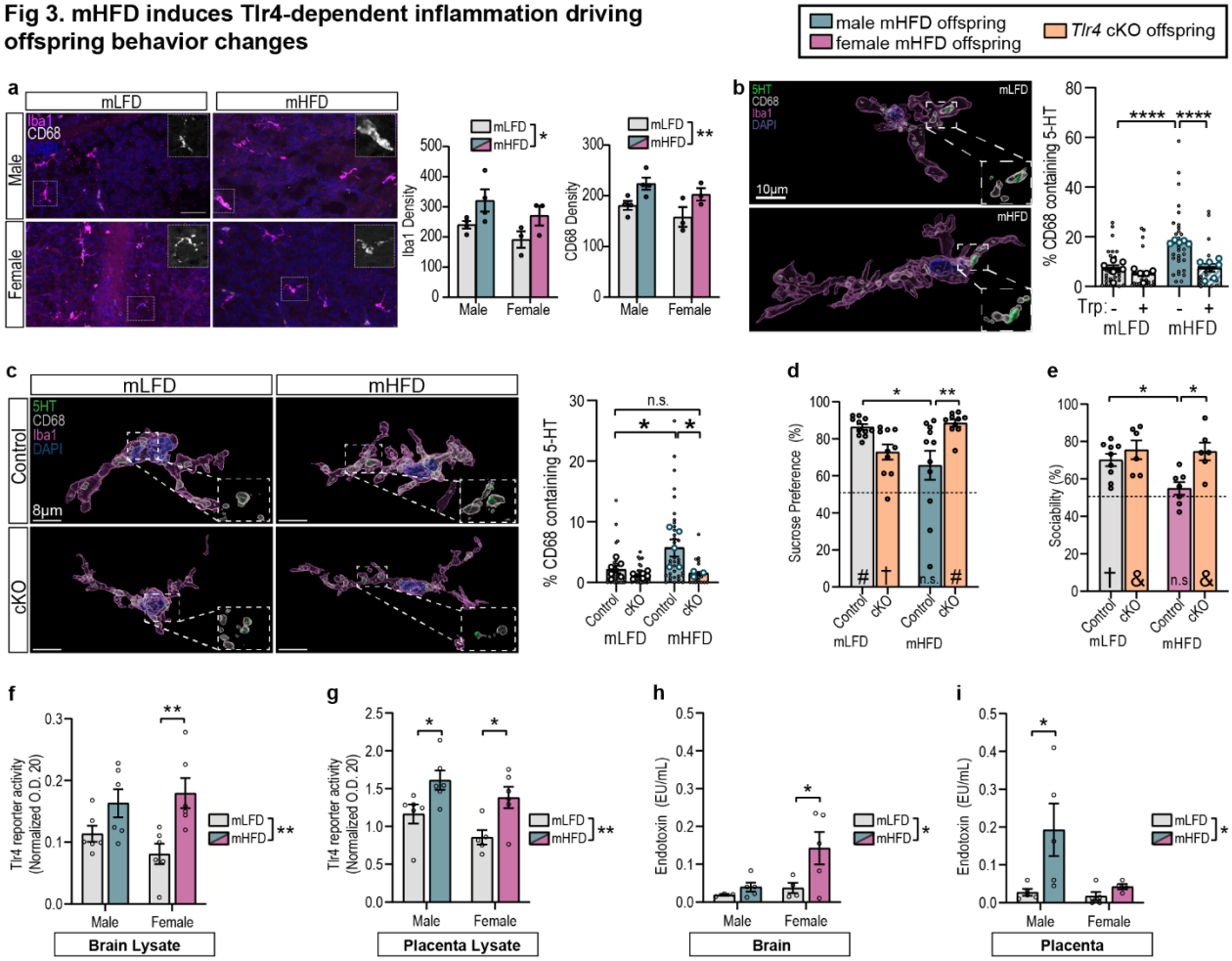

a, Increased microglia and phagosome immunoreactivity in male and female mHFD DRN at e14.5 (scale=50µm; n=4 male and 3 female/diet from 3mLFD and 3mHFD litters). **b,** IMARIS reconstructions of DRN microglia reveals increased microglial phagocytosis of serotonin in males at e14.5. Statistics are displayed for animal average (large circles), small circles are individual microglia reconstructions (n=6 mLFD, 5mLFD+Trp, 5 mHFD, 6 mHFD+Trp mice from 3 mLFD, 2 mLFD+Trp, 3 mHFD, and 3mHFD+Trp litters). **c,** IMARIS reconstruction of DRN microglia in male control and *Tlr4* cKO e14.5 offspring (n=6 mLFD control, 6 mLFD cKO, 5 mHFD control, and 3 mHFD cKO male offspring from 7 mLFD and 5 mHFD litters). **d,** Decreased sucrose preference is rescued in male mHFD offspring lacking macrophage-Tlr4 signaling. (n=11 mLFD, 10 mLFD cKO, 11 mHFD, and 10 mHFD cKO from 5 mLFD and 6 mHFD litters). **e,** Decreased social preference is rescued in female mHFD offspring lacking macrophage-Tlr4 signaling. (n=9 mLFD, 6 mLFD cKO, 7 mHFD, and 6 mHFD cKO from 5 mLFD and 5 mHFD litters). **f-g**, Tlr4-reporter activity in response to e14.5 brain (f) and placenta (g) lysate from mLFD and mHFD offspring (n=6 offspring/sex/diet from 5 mLFD and 5 mHFD litters). **h-i**, Endotoxin levels in mLFD and mHFD brain (h) and placenta (i) tissue lysate (n=3-5 mLFD male, 4-5 mLFD female, 5 mHFD male, 4-5 mHFD female from 5 mLFD and 5 mHFD litters). Data are mean ± s.e.m.; asterisk denoted p-values are derived from two-way ANOVA (**a-i**). other p-values (# $p<0.0001$, † $p<0.001$, & $p<0.01$) are derived from one-sample t-tests assessing difference from chance (50%) (**d, e**). n.s. not significant

286 generated a conditional Tlr4 knock-out mouse (cKO) line using Cx3cr1-Cre BAC-
287 transgenic[51] and Tlr4$^{f/f}$ mice[52] (Extended Data Fig 7f). Female control (*Tlr4*$^{f/f}$) mice were
288 transitioned to HFD for six weeks, then subsequently mated to male *Cx3cr1-Cre;Tlr4*$^{f/f}$
289 mice to generate control and cKO mHFD offspring. qPCR revealed significant (~95%)
290 knockdown of *Tlr4* in cKO microglia (Extended Data Fig 7f). 5-HT was increased in male
291 fetal forebrain and adult midbrain in mHFD cKO offspring (Extended Data Fig 7g-i).
292 IMARIS reconstructions of mLFD and mHFD microglia from control and *Tlr4* cKO e14.5
293 DRN revealed a significant rescue of 5-HT phagocytosis by microglia in mHFD *Tlr4* cKO
294 male offspring (Fig 3c). No significant changes were detected in females (Extended Data
295 Fig 7j). Loss of *Tlr4* decreased USV similarity in male mLFD offspring while increasing it
296 in male mHFD offspring (Extended Data Fig 8a), suggesting a role for macrophage *Tlr4*
297 signaling in USV behavior independent of maternal dietary fat composition. In male mHFD
298 offspring, loss of *Tlr4* completely rescued mHFD-induced anhedonia (Fig 3d, Extended
299 Data Fig 8c), and did not influence male social preference (Extended Data Fig 8d).
300 Interestingly, female mHFD *Tlr4* cKO offspring did not display a preference for sucrose
301 (Extended Data Fig 8e), suggesting that increased Tlr4 signaling in female mHFD
302 offspring may be preventing anhedonia. *Tlr4* knockdown partially rescued the number of
303 USVs, but did not rescue total call time, or mean call length in male mHFD cKO offspring
304 (Extended Data Fig 8a), suggesting that different USV metrics may be driven by different
305 mechanisms. Corroborating this, in female mHFD cKO offspring, we saw significant
306 improvement of USV similarity (Extended Data Fig 8b) but no change in the number of
307 USVs. *Tlr4* cKO resulted in a partial rescue of total call time, inter-syllable interval, and
308 mean syllable number in female mHFD cKO mice, but no rescue of mean call length or

309 mean frequency (Extended Data Fig 8b). Juvenile female mHFD cKO offspring showed
310 a complete rescue of social preference (Fig 3e, Extended Data Fig 8f), suggesting that
311 mHFD-induced *Tlr4*-dependent inflammation in females is responsible for most
312 behavioral outcomes, through a non-5-HT mechanism.

313 To understand how mHFD results in activated Tlr4 signaling in fetal tissue, we
314 used a Tlr4-reporter cell line (HEK-Dual™ mTLR4 (NF/IL8), Invivogen) to determine if
315 mHFD tissue lysate stimulates Tlr4 signaling. Application of lysate from mLFD and mHFD
316 placenta and brain tissue revealed robust Tlr4 activation in response to mHFD versus
317 mLFD tissue (Fig 3f-g). As dietary fats reach the fetus through the placenta, and some
318 literature suggests that saturated fatty acids (SFAs) stimulate Tlr4 signaling[53], we
319 determined if the increased SFAs in our model could directly activate Tlr4 signaling by
320 stimulating the reporter cell line with six SFAs that were most abundant (and most
321 increased) in our HFD model. While stearic acid was able to significantly activate Tlr4
322 signaling, as previously described[54], the magnitude of the response was minimal
323 (Extended Data Fig 7k).

324 Previous literature has demonstrated that pre-gravid obesity and high-fat diet
325 increase circulating endotoxin levels[55–57], and that LPS injected into pregnant dams can
326 reach fetal tissue[58]. As Tlr4 is classically activated by bacterial endotoxins, we
327 hypothesized that mHFD offspring tissue may be exposed to and accumulate endotoxin.
328 Thus, we quantified bacterial endotoxin presence by limulus amebocyte lysate (LAL)
329 assay. We detected significantly more endotoxin in mHFD placenta and fetal brain tissue
330 from male and female offspring (Fig 3h-i), suggesting that mHFD increases endotoxin
331 load in fetal tissue and activates Tlr4 signaling.

332 **Maternal overnutrition causes decreased prenatal 5-HT in human male brain tissue**

333 To determine to what degree our findings are translatable to the human population,
334 we obtained a large (37 individuals) cohort of matched tissues (fetal brain, fetal placenta,
335 and maternal placenta (decidua)) from fetuses collected via elective termination at 72-82
336 days post conception (d.p.c.), a timeframe that closely matches the embryonic
337 developmental window used in our mouse studies (14.5-16.5 d.p.c.; Fig 4a). PCR for the
338 Y chromosome (*SRY;* Supplementary Table 2) identified 17 male and 20 female fetal
339 tissue sets, with the average age of 78.2 d.p.c. for both sexes (Extended Data Fig 9a).
340 No maternal data were available, so we assessed if triglyceride accumulation in the
341 placenta could serve as a proxy for maternal dietary fat consumption, given that in
342 humans, placental triglyceride/lipid levels have been shown to be increased in the context
343 of maternal obesity[59–61]. To show proof of principle in our mouse model, triglyceride
344 measurements from mLFD and mHFD placenta revealed a significant increase in
345 triglyceride levels in mHFD offspring placenta, in agreement with previous literature[62]
346 (Extended Data Fig 9b), and placental triglyceride levels were significantly negatively
347 correlated with fetal brain 5-HT in males (Extended Data Fig 9c). Thus, in the human
348 samples, we assessed decidual triglyceride accumulation to use as a proxy for maternal
349 dietary fat consumption. Triglyceride levels trended higher in pregnancies with female
350 fetuses, but there was no significant difference between triglyceride accumulation in
351 decidua associated with male or female pregnancies (Extended Data Fig 9d). Correlation
352 of gene expression with maternal triglyceride accumulation from bulk RNA-seq from 16
353 matched male and 19 matched female brain and placenta samples revealed a strong
354 dimorphic trend in gene expression. In male placenta, differentially correlated genes were

355 predominantly over-expressed with increasing maternal triglycerides (i.e. gene
356 expression increased as maternal triglycerides increased); notably, the opposite effect
357 was seen in female placenta (Fig 4b). In the male brain, only 45 genes significantly
358 correlated with maternal triglyceride accumulation (either positive or negative), whereas
359 781 genes were significantly correlated in female brain tissue (Fig 4b). At collection, the
360 entire fetal brain tissue was collected and thus we could not control for region-specificity.
361 To address this, we used the Allen Brain Atlas Developmental Human Transcriptome
362 (https://www.brainspan.org/) to identify marker genes for major brain regions in human
363 development (8-12 weeks post conception) and we plotted their gene expression
364 (Extended Data Fig 9e). The majority of our samples showed consistent gene expression
365 across all brain regions (i.e. one region was not oversampled). Gene Ontology (GO)
366 Enrichment Analysis of genes significantly positively correlated with maternal triglyceride
367 accumulation revealed enrichment of inflammatory signaling pathways in both male and
368 female placenta (Fig 4c; full GO enrichment data is available in Supplementary Table 1).
369 Correlation analyses of targeted genes reinforced these pro-inflammatory phenotypes;
370 assessment of common macrophage, trophoblast and syncytiotrophoblast markers[63]
371 revealed specific gene associations predominantly within macrophages (Extended Data
372 Fig 9f, Fig 4b). In agreement with our findings in mice, *TLR* expression was positively
373 correlated with maternal triglyceride accumulation in males, along with several genes
374 associated with MyD88-independent TLR4 signaling (Extended Data Fig 9f). In males,
375 GO enrichment from placental genes that were negatively correlated with maternal
376 triglycerides revealed a pattern of repressive cell differentiation, particularly of immune
377 cells (e.g. RUNX1 differentiation and myeloid cell differentiation). That is, with increasing

378 maternal triglyceride accumulation, gene expression of factors important for cell
379 differentiation decreased (Fig 4c). In females, placental genes that were negatively
380 correlated with maternal triglycerides were often involved in vascular growth and
381 development, suggesting that maternal triglyceride accumulation may decrease placental
382 vasculogenesis/angiogenesis (Fig 4c), an important finding given that changes in the
383 placental vascular network are associated with numerous pathologies, such as
384 preeclampsia[64,65]. Inflammatory responses were additionally enriched in female brain
385 (e.g. response to TGF-β), but too few genes were correlated in males to determine if this
386 association was true independent of sex. These inflammatory transcriptomic patterns
387 support our findings in mice that male mHFD offspring primarily accumulate endotoxin in
388 placental tissue, whereas female mHFD offspring primarily accumulate endotoxin in brain
389 tissue (see Fig 3h-i). Lastly, the top GO enrichment categories from female brain
390 transcripts negatively correlated with maternal triglyceride accumulation involved
391 neuronal development (Fig 4c), suggesting that maternal high-fat diet and accompanying
392 fetal inflammation may impede brain development.

393 Finally, to determine if 5-HT levels were impacted by maternal triglyceride
394 accumulation, we assessed 5-HT in human male and female fetal brain and placenta.

Fig 4. Maternal triglycerides negatively correlate with male fetal brain 5-HT

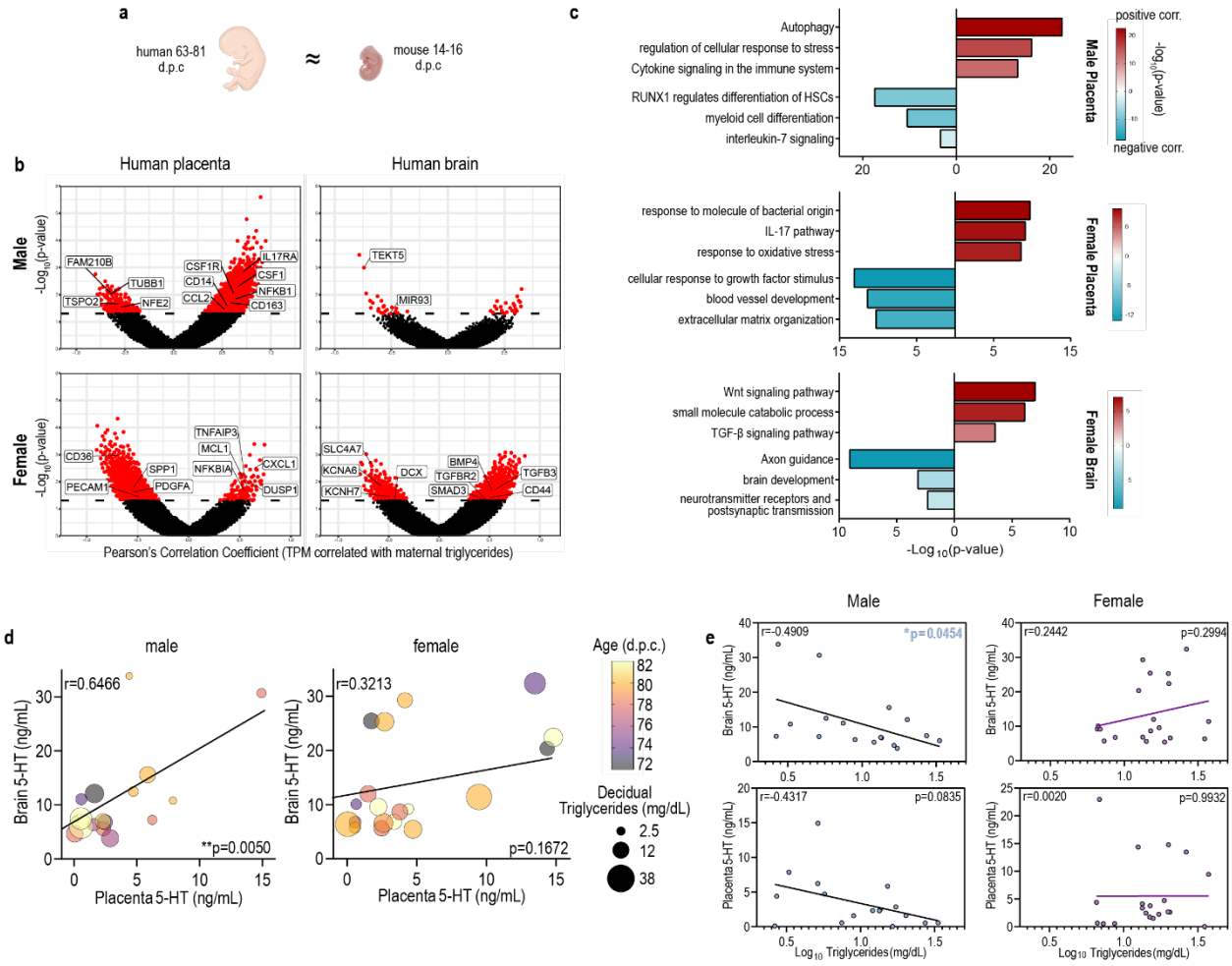

a, Human fetal development at 63-81 days post conception (d.p.c.) is roughly equivalent to mouse embryonic development at 14-16 d.p.c. **b,** Scatter plots showing transcript (TPM) correlation with maternal triglycerides versus -Log_{10}(p-value) in male and female placenta and brain bulk sequencing data (n=16 matched male tissue sets, 19 female). Red dots indicate a significant p-value (<0.05). **c,** GO Enrichment analysis of transcripts significantly correlated with maternal triglyceride accumulation demonstrates robust and distinct upregulation in immune responses in male and female placenta in response to increasing maternal triglyceride accumulation. GO enrichment of transcripts significantly correlated with maternal triglyceride accumulation shows downregulation of neuronal development and function in female brain tissue in response to increasing maternal triglyceride accumulation. **d,** Multivariate dot plots show Pearson correlations between brain and placental serotonin from male and female human fetal tissues. Dot color represents the age of the matched tissue set, and dot size represents the maternal decidual triglyceride level (mg/dL), a proxy for maternal dietary fat intake. Brain and placental serotonin levels are significantly positively correlated in male tissues between 72 and 82 d.p.c. Brain and placental serotonin levels are not correlated in female tissues (n=17 matched male tissue sets, 20 female). **e,** Brain serotonin levels are significantly negatively correlated with decidual triglyceride levels in males only. Placental serotonin levels trend towards a negative correlation with decidual triglycerides in males only. Data are mean ± s.e.m.; n represents biologically independent matched human tissue set. asterisk denoted p-values are derived from Pearson's correlations.

Correlation analyses revealed a significant positive correlation between placental and brain 5-HT only in male fetal tissues (Fig 4d). This is consistent with previous literature (sex not reported)[30] and our findings in male mice (see Fig 2e, Extended Data Fig 5f). Importantly, brain region marker gene expression did not correlate with 5-HT levels, and the top samples that most overrepresented midbrain gene expression profiles did not drive the correlation. Correlation analyses further revealed a negative correlation between

402 brain or placental 5-HT levels and maternal triglyceride accumulation in male tissue only
403 (Fig 4e). This is in agreement with our findings in mice that mHFD results in decreased
404 brain and placental 5-HT levels in male fetal tissue (see Fig 2a-b, Extended Data Fig 4d-
405 e). In sum, in both mice and humans, maternal high-fat diet results in the perpetuation of
406 inflammation to the fetal brain and placenta in both sexes. In males, this inflammatory
407 response results in aberrant phagocytosis of 5-HT neurons and long-lasting decreased
408 levels of brain 5-HT and decreased reward behavior.

409 **Discussion**

410 Here, we demonstrate a fundamental, sex-biased mechanism through which maternal
411 high-fat diet increases offspring susceptibility to neuropsychiatric disorder development.
412 Our results demonstrate that, in the context of maternal high-fat diet, endotoxin
413 accumulation mediates *in utero* inflammation through the pattern recognition receptor Tlr4
414 in males and females, leading to increased macrophage reactivity in both the placenta
415 and the fetal brain. In female mice, Tlr4-dependent inflammation causes diminished social
416 preference through a 5-HT-independent mechanism. In human females, maternal
417 decidual triglyceride accumulation is negatively associated with brain development,
418 suggesting that Tlr4-dependent inflammation impacts neuronal development in females,
419 though the target neuronal population is not yet known. In male mHFD offspring,
420 embryonic microglia aberrantly phagocytose 5-HT neurons in the DRN, leading to
421 diminished brain 5-HT from embryonic stages through adulthood, and offspring
422 anhedonia. In human males, maternal decidual triglyceride accumulation is associated
423 with pro-inflammatory signaling pathways in both sexes, and negatively correlated with
424 brain 5-HT levels in males only, reinforcing our findings in mice.

425 Seminal work reported the placenta as a transient source of 5-HT for the fetal
426 brain[30], though recent studies suggest that the fetal placenta lacks the enzymes required
427 for 5-HT synthesis[46]. No studies have investigated whether fetal sex plays a role in 5-HT
428 synthesis or transfer in the placenta. Further, whether developmental 5-HT levels are
429 reflective of adult 5-HT levels, and if disruptions to 5-HT levels during this window impact
430 the brain long-term are unknown. Here, we show that fetal placenta and brain 5-HT levels
431 are susceptible to perinatal inflammation in males only, and that decreased fetal 5-HT
432 levels are reflective of decreased adult brain 5-HT levels in the context of maternal high-
433 fat diet. We further found that transcript levels of both the neuronal 5-HT synthesis
434 enzyme and 5-HT transporter (*Tph2* and *5HTT*, respectively) were decreased in male
435 mHFD placenta, but we did not distinguish between the maternal and fetal compartments
436 of the placenta. By manipulating fetal 5-HT levels through maternal dietary tryptophan
437 enrichment, we can shed light on the relationship between placental and fetal brain 5-HT.
438 While at baseline there is a significant positive correlation between placental and fetal
439 brain 5-HT in males only, maternal tryptophan supplementation disrupted the correlation.
440 This suggests that either the placenta is not the sole source of fetal brain 5-HT, or that
441 the fetal brain is capable of sensing and limiting the influx of placental 5-HT in cases of
442 excess. Alternatively, maternal dietary changes may alter the timing of the switch from
443 placental 5-HT dependence to fetal midbrain 5-HT dependence. Careful investigation of
444 the spatiotemporal expression of placental 5-HT transport and synthesis enzymes in male
445 and female placenta and decidua is warranted to further clarify this topic.
446 5-HT has been postulated to influence macrophage phagocytic activity and cytokine
447 production for decades[66,67]. Here, we demonstrate a novel male-specific potential

448 feedback loop through which microglial phagocytosis influences central 5-HT levels,
449 which in turn influence microglial phagocytic activity. mHFD results in increased
450 inflammation dependent on macrophage Tlr4 signaling, which results in microglial over-
451 phagocytosis of 5-HT neurons in the DRN of males only. Considering 5-HT is thought to
452 decrease phagocytic capacity[43], this resulting decrease in 5-HT thus propagates the over-
453 phagocytosis of the mHFD microglia. Both abrogation of overactive Tlr4-signaling in
454 macrophages and increased 5-HT bioavailability via maternal tryptophan
455 supplementation were sufficient to rescue central 5-HT levels, demonstrating the
456 reciprocal relationship between inflammation and 5-HT in the male fetal brain.

457 In closing, mechanisms through which chronic maternal inflammation impact
458 offspring neurodevelopment are scarce. In our mouse model, we demonstrate that fetal
459 inflammation is propagated by macrophage-specific Tlr4 in both male and female mHFD
460 offspring, along with sex-specific neurodevelopmental and behavioral outcomes. Further,
461 we generated a large sequencing dataset of human fetal tissue from both male and
462 female pregnancies, which demonstrated 1) a high degree of fetal inflammation in both
463 male and female placenta, and particularly in female brain in response to increasing
464 maternal triglyceride accumulation, and 2) sex-specific inflammatory responses. These
465 data will shed light on which other fetal inflammatory pathways might be responsive to
466 maternal triglyceride accumulation and will provide direction for future studies.

467 **Methods**

468 **Animals:** All procedures relating to animal care and treatment conformed to Duke
469 Institutional Animal Care and Use Committee (IACUC) and NIH guidelines. Animals were
470 group housed in a standard 12:12 light-dark cycle. The following mouse lines were used

471 in this study: *C57BL/6J* (Jackson Laboratory, stock no. 000664), *C57BL/6NCrl* (Charles
472 River, #027), Cx3cr1-Cre BAC-transgenic[51], *Tlr4*$^{f/f}$ (JAX 024872[52]). Cx3cr1-Cre mice were
473 developed in *C57BL/6N* mice but have been backcrossed with *C57BL/6J* mice for multiple
474 generations. The Cre transgene was maintained in males for all experimental studies.
475 Jackson Labs maintains the *Tlr4*$^{f/f}$ mice on a *C57BL/6J* background, though single
476 nucleotide polymorphism (SNP) analysis suggests that the original mice provided to JAX
477 were a mixed *C57BL/6N;C57BL/6J* strain. Our in-house breeding has backcrossed them
478 with *C57BL/6J* for multiple generations.

479 **Diets:** Female *C57BL/6J* mice were placed on randomly assigned diet at 4-weeks old
480 and given *ad libitum* access to their assigned diet chow and water. Weight gain was
481 assessed three times/week. After 6-weeks on diet, females were mated with *C57BL/6J*
482 males. Pregnancy was determined by the presence of a copulation plug (gestational day
483 0.5) and maternal weight was assessed daily. Dams were maintained on their assigned
484 diet chow throughout gestation and until the pups were weaned. At weaning, offspring
485 were group housed with sex-matched littermates and provided *ad libitum* access to rodent
486 chow 5001 (standard rodent chow, 13% kcal from fat). Low-fat, high-fat, low-
487 fat+tryptophan, and high-fat+tryptophan diets were purchased from Research Diets (low
488 fat: D12450Hi, high-fat: D12451i). Tryptophan enriched diets were custom formulations
489 resulting in 1% final tryptophan content.

490 **Tissue Collection and Analyses:** *Murine Tissue collection:* Pregnant dams were
491 euthanized using CO_2 following Duke University Animal Care and Use guidelines. Uterine
492 horns were dissected and placed on ice in sterile 1X PBS. Individual embryos were
493 separated, and placenta, brain, and tail tissue (for genotyping) were collected. Placenta

494 were dissected into three equal pieces. One piece was flash-frozen in liquid nitrogen at
495 stored at -80°C until ELISA. One piece was placed into 4% paraformaldehyde in PBS
496 (PFA, Sigma) for immunohistochemistry (IHC). The final piece was placed in TriZol and
497 stored at -80°C. Dissected fetal brains were cut in half coronally; fetal forebrain tissue
498 was flash frozen for ELISA while the remainder of the brain was placed into 4% PFA for
499 IHC. For adult brain collections, offspring were anesthetized with CO_2 and transcardially
500 perfused with saline. Further dissections were done to isolate the midbrain, and brain
501 tissues were immediately flash frozen in liquid nitrogen and stored at -80°C until
502 processing.

503 *Microglia isolation:* Microglia were isolated using CD11b-beads as previously described[68].

504 *Human tissue collection:* Human placenta (maternal decidua separated from fetal
505 placenta) and fetal brain tissues were obtained from the NIH-supported (5R24HD000836)
506 Laboratory for the Study of Embryology at the University of Washington, Seattle between
507 the years 1999 and 2010 and used under a protocol approved by the Duke University
508 Institutional Review Board (Pro00014066). Fetuses with known chromosomal
509 abnormalities were not collected. At the time of collection, tissue specimens were placed
510 in cryogenic tubes and immediately frozen on dry ice and stored at -80°C until required
511 for RNA or protein extraction. Prior to collection, informed consent was obtained from all
512 individuals undergoing the elective termination.

513 *Immunohistochemistry:* Placenta and brain tissue were fixed in 4% PFA overnight at 4°C,
514 cryoprotected in 30% sucrose + 0.1% sodium azide in PBS (Sigma), and embedded in
515 OCT (Sakura Finetek, Torrance, CA) before being cryo-sectioned directly onto Superfrost
516 slides (Fisher) at 40μm. Sections were frozen at -20°C for storage. For IHC, sections were

517 permeabilized in 1% Triton X-100 in PBS for 12 minutes, blocked at room temperature
518 (RT) with 5% goat serum (GS) in PBS + 0.1% Tween-20, then incubated for 2 nights at
519 4°C with chicken anti-Iba1 (Synaptic Systems, 234 006) or goat anti-Iba1 (Novus, NB100-
520 1028), rat anti-CD68 (Biolegend, 137002), and rabbit anti-5-HT (Sigma, S5545) or rat
521 anti-F4/80 (Abcam, ab6640). Sections were then washed with PBS and incubated in the
522 following secondary antibodies: anti-rabbit Alexa-488, anti-chicken Alexa-647 or anti-goat
523 Alexa-647, and anti-rat Alexa-568 (brain), or anti-rat Alexa-568 (placenta; 1:200;
524 ThermoFisher), and DAPI (100µg/mL). Ten z-stacks of 0.5µm optical thickness were
525 taken at 20X using a Zeiss AxioImager.M2 (with ApoTome.2) from at least 5 sections
526 (each 400µm apart) from the fetal compartment of each placenta for F4/80+ cell
527 quantification. Ten z-stacks of 0.5µm optical thickness were also taken at 20X from at
528 least 3 fetal brain sections/animal (each section being 200µm apart) for Iba1 and CD68
529 immunoreactivity. For IMARIS reconstructions, z-stacks of 0.25µm optical thickness were
530 taken to capture entire microglia. Surface reconstructions of Iba1, CD68, 5-HT, and DAPI
531 were done for at least 19 microglia/diet from 6 mLFD, 5mLFD+Trp, 5 mHFD, and 6
532 mHFD+Trp male offspring and at least 12 microglia/diet from 3 mLFD, 5 mLFD+Trp, 6
533 mHFD, and 5 mHFD+Trp female offspring (3 litters/diet). Reconstructions from were done
534 for at least 16 microglia/diet from 6 mLFD control, 6 mLFD cKO, 5 mHFD control, and 3
535 mHFD cKO male offspring and 7 mLFD control, 5 mLFD cKO, 5 mHFD control, and 4
536 mHFD cKO female offspring from 7 mLFD and 5 mHFD litters. Slides with cryosectioned
537 tissue were de-identified and the individual performing the IHC, imaging, and image
538 analyses was blind to sex, genotype, and maternal diet at all times. Statistics were run on
539 animal average values, not individual microglia values.

540 *5-HT ELISA*: Mouse placenta and brain tissue were thawed on ice and homogenized in
541 freshly prepared lysis buffer (final concentrations: 1mg/mL ascorbic acid, 0.147% NP-40,
542 1X HALT Protease Inhibitor (Thermo 78443) in 1X PBS). Samples were then centrifuged
543 at 13,000 xg for 20 minutes; supernatant was diluted 1:2 for placenta, or undiluted for
544 fetal brain preparations, and loaded and processed according to manufacturer
545 instructions (Enzo, ADI-900-175). Dam blood was collected in heparinized capillary tubes
546 and immediately transferred to Eppendorf tubes on ice before being centrifuged at 1.6 x
547 1000 rpm for 20 minutes at 4°C. Plasma was stored at -80°C for a maximum of 2 weeks
548 before assessment for 5-HT according to manufacturer's instructions (1:16 dilution).
549 *Quinolinic Acid/Kynurenic Acid ELISA*: Mouse placenta and brain tissue were thawed on
550 ice and homogenized with Dounce homogenizers in 500µL 1X PBS with 1X HALT
551 Protease Inhibitor. Samples were then centrifuged at 13,000 xg for 10 minutes and
552 supernatant processed according to manufacturer instructions (ImmuSmol IS I-0200, IS
553 I-0100).
554 *Decidual Triglycerides*: Human decidua samples (stored at -80°C) were kept on dry ice
555 to remove ~150mg tissue which was then thawed on ice, and homogenized in 1mL NP40
556 Substitute Assay Reagent (Cayman Chemical, 10010303). Homogenized samples were
557 centrifuged at 10,000 xg for 10 minutes at 4°C and the supernatant was processed
558 (undiluted) according to manufacturer instructions at room temperature (Cayman
559 Chemical, 10010303). Mouse placenta samples (stored at -80°C) were thawed on ice and
560 ~40mg of tissue was homogenized in 500µL NP40 Substitute Assay Reagent.
561 Homogenized samples were centrifuged at 10,000 xg for 10 minutes at 4°C and the

562 supernatant was processed (undiluted) according to manufacturer instructions at room
563 temperature (Cayman Chemical, 10010303).
564 *High-performance liquid chromatography (HPLC) with electrochemical detection*: Female
565 *C57BL/6NCrl* (Charles River #027) mice were placed on LFD or HFD as described above,
566 with the exception that these diets were not irradiated. Pregnant females were euthanized
567 at gd14.5 by lethal i.p. injection with ketamine/xylazine. Placentae were separated from
568 each fetus, the amniotic sac and maternal membranes were removed, and the resulting
569 discoid placenta was cut in half sagitally. One half was snap-frozen in liquid nitrogen for
570 HPLC analysis. Fetal brains were dissected and snap-frozen in liquid nitrogen as well.
571 Placenta and brain samples were analyzed for 5-HT, the 5-HT precursor tryptophan (Trp),
572 and the 5-HT metabolite 5-hydroxyindoleacetic acid (5-HIAA). On the day of analysis,
573 500µl of ice-cold standard buffer (0.5 mM sodium metabisulfite, 0.2 N perchloric acid, and
574 0.5 mM EDTA) was added to thawed (on ice) placenta tissue and 250µl was added to
575 thawed brain tissue. Tissues were then disrupted by sonication until completely
576 homogenized, then centrifuged at 16,000 x g for 10 min at 4°C. The supernatant was
577 collected and filtered through a 0.45µm membrane via centrifugation (Durapore PVDF
578 centrifugal filters, Millipore, Billerica, MA, USA). The filtrate was kept on ice until analysis.
579 Processed samples were separated using a 100 x 4.6 mm Kinetex (C18 5 µm 100 Å,
580 Phenomenex) column on a reverse-phase HPLC system with a BAS LC-4B
581 electrochemical detector with dual 3mm carbon electrode (MF-1000) and reference
582 electrode (MF-2021) as previously described[69]. An external standard curve of all analytes
583 was run each day. Trp quantification was performed using a mobile phase consisting of
584 8% acetonitrile (v/v), 0.05 M citric acid, 0.05 M Na2HPO4•H2O, and 0.1 mM EDTA. No

585 correction for pH was needed. The detector was set to 0.875 V versus Ag/AgCl reference
586 electrode, sensitivity at 20 nA, and a flow rate of 1.0 ml/min. 5-HT and 5-HIAA were
587 separated with a mobile phase consisting of 18% methanol (v/v), 0.1M sodium phosphate,
588 0.8 mM octanesulfonic acid (anhydrous), and 0.1 mM EDTA (final pH adjusted to 3.1).
589 The detector was set to 0.70 V, sensitivity at 20 nA, and a flow rate of 1.0 ml/min.
590 *Limulus amebocyte lysate (LAL) assay for endotoxin detection*: Fetal placenta and brain
591 tissue from e14.5 mLFD and mHFD offspring were collected in a sterile environment and
592 frozen in the vapor phase above liquid nitrogen before being transferred to 2mL
593 Eppendorf tubes and being stored at -80°C to prevent endotoxin leaching into the tubes.
594 The day before sampling for endotoxin, the samples were rapidly transferred to glass
595 Dounce homogenizers and homogenized in 750µL of endotoxin free water (Lonza W50-
596 100). Homogenized samples were then diluted 1:5 in endotoxin free water in pyrogen-
597 free glass tubes (Lonza N207) and tested for endotoxin in duplicate using a Kinetic-
598 QCL™ LAL Assay (Lonza, 50-650U) according to manufacturer's instructions and
599 including a third 'spiked' sample from each tissue (5EU/mL endotoxin added) to ensure
600 acceptable recovery from every sample. Plates were run on a kinetic SPECTROstar Nano
601 (BMG Labtech) plate reader and analyzed with MARS data analysis software (BMG
602 Labtech) with a baseline correction of ΔO.D.=0.2[70]. Samples in which the 'spiked' sample
603 fell outside the acceptable recovery range were excluded (two samples in total).
604 **Behavior:** Behaviors are presented sex-stratified as they are often sex-dependent in their
605 presentation[71,72].
606 *Ultrasonic Vocalizations (USVs)*: At P8, pups were brought in their home cage (with the
607 dam being the only adult in the cage) to the testing room. Each pup was removed from

608 their home cage and placed directly in a small cup in an insulated chamber with an AviSoft
609 Condenser ultrasound microphone (Avisoft-Bioacoustics CM16/CMPA) suspended four
610 inches above the contained pup. The dam and any remaining littermates were removed
611 from the testing room in the home cage. After 3 minutes of recording, pups were weighed
612 and sexed before being returned to their home cage. After the dam attended to each
613 returned pup, the home cage was returned to the colony room. USV analysis was done
614 with Avisoft and MUPET[23] (Mouse Ultrasonic Vocalization Extraction Tool). Default
615 MUPET parameters were used with the exception of: noise-reduction = 8.8, minimum-
616 syllable-duration = 2.0, as we have previously optimized[39]. 80-unit repertoires were
617 generated for each dataset (e.g. all male mLFD calls from one cohort were combined to
618 generate ranked syllable units by frequency of occurrence) and manually inspected
619 before USV similarity was determined using MUPET. USV similarity represents an overall
620 Pearson's rank order comparison of individual repertoire units (RUs) across datasets
621 based on their spectral shape[23].

622 *Open Field Test:* Adult offspring were placed in a 50cm x 50cm square enclosure with
623 38cm high walls and allowed to explore freely for ten minutes[73]. Behaviors were recorded
624 and analyzed using EthoVision video tracking software (Noldus). Center-avoidance was
625 assessed by comparing time spent at the periphery to time spent centrally/number of
626 central entries (middle third of chamber).

627 *Sociability/Social Novelty Preference*: Mice were assessed for social preference or social
628 novelty preference using a classic 3-chambered social preference test[74]. One day prior
629 to testing, subject and stimulus animals were habituated to the testing room for a minimum
630 of 1 hour before being individually habituated to the 3-chambered social preference boxes

631 for 5 minutes each. On test day, subject and stimulus animals were habituated to the
632 testing room for a minimum of one hour before testing. Juvenile offspring were tested for
633 preference to interact with either a novel age- and sex-matched conspecific or an
634 inanimate novel object (rubber duck). Mice were placed in the middle chamber with the
635 inanimate object confined in a clear plexiglass cylindrical cage (plexiglass rods for
636 thorough cleaning) on one side of the test and a novel conspecific confined in an identical
637 cage on the other side for 5 minutes. The inanimate object was then replaced with a new
638 novel age- and sex-matched conspecific and experimental animals were allowed to freely
639 investigate either the new animal or the familiar animal. The entire 10-minute test was
640 recorded with a Logitech webcam, and all behavior was manually quantified using
641 Solomon Coder by an observer blind to sex/treatment. The time spent, latency to first
642 instance, and frequency of each of the following behaviors was coded: in chamber,
643 investigating (nose poking into the cage), and climbing (front paws on cup and back fully
644 extended/arched or on top of the cage). A mouse was considered “in” a chamber after its
645 head crossed the threshold from one chamber to the next. Mice that spent >20% of the
646 test climbing were excluded from analysis. Mice were also excluded from analysis if they
647 did not enter any one of the three chambers, or if the latency to enter any one chamber
648 was greater than 150s (half the test). Social preference is represented by a sociability
649 score significantly higher than chance (50%). Sociability score formula: (time investigating
650 social stimulus/ (total investigation time (social + object))*100). Social Novelty Preference
651 score formula: (time investigating novel social stimulus/ (time investigating novel +
652 familiar social stimuli))*100).

653 *Sucrose Preference:* Adult offspring were tested for their preference for a 1% sucrose
654 solution in water or plain water. Mice were singly housed and provided with 2 drinking
655 bottles and extra enrichment (toy block or bone) for a total of 6 days. After 3 days
656 (acclimation to 2 bottles with drinking water in both), one bottle was filled with a 1%
657 sucrose solution while the other was filled with drinking water. Sucrose and water intake
658 were measured daily (by weight) over the next 3 days. The positions of the bottles were
659 switched daily to reduce any bias in side-preference. Sucrose preference is calculated as
660 ((sucrose intake)/(sucrose + water intake))*100) averaged over 3 days.
661 *Forced Swim Test*: Adult offspring were assessed for mobility behavior in a forced-swim
662 test (FST). Individual mice were placed in a cylindrical container (20cm in diameter x
663 50cm high) filled 2/3 with water (26°C-30°C) for 7 minutes. Mice were monitored via
664 webcam for the testing period, and mice were removed from the test early (and not used
665 for analysis) if their head dipped fully below the water at any point. After the test period,
666 animals were moved to an enclosure with a small towel and heating pad to dry. Time
667 spent time immobile (not swimming or climbing) was quantified using Solomon Coder by
668 an observer blind to sex/treatment. Velocity and distance moved were quantified by
669 EthoVision XT tracking software (Noldus).
670 **qRT-PCR:** RNA was isolated using TRIzol RNA extraction reagent chloroform extraction.
671 Either 1µg (placenta) or 200-250ng (isolated microglia) RNA was reverse-transcribed into
672 cDNA using a Qiagen QuantiTect Reverse Transcription kit (205311). qPCR was
673 performed on an Eppendorf Realplex ep Mastercycler using Sybr/Rox amplification with
674 a QuantiFAST PCR kit (204056). Primer sequences are listed in Supplementary Data
675 Table 2. Fold change was calculated using the $2^{(-\Delta\Delta CT)}$ method with 18S as an

676 endogenous control. When transcripts were not detected a CT value of 40 (max cycle
677 number) was assigned to that sample. *Trem2* was largely undetected in e14.5 microglia
678 (~40% of samples equally between male and female mLFD and mHFD microglia) and is
679 thus not represented in Extended Data Fig 7b).

680 **Sequencing**: RNA from human tissue was prepared for sequencing using an Illumina
681 TrueSeq RNA Exome kit and sequenced on an Illumina NovaSeq 6000 configured for a
682 S2 flow cell at 50bp PE. Brain and placenta count matrices were processed separately.
683 Reads were aligned to the human genome using Bowtie2[75]. Transcripts per million (TPM)
684 was calculated on the raw counts and used for all subsequent analyses. Gene inclusion
685 was determined using EgeR[76] (threshold of 1). Pearson's correlation coefficients and p-
686 values were calculated for each gene (TPM correlated with log10(maternal triglyceride
687 accumulation)), and data was plotted in a volcano plot using custom R script. All code for
688 processing is currently hosted and publicly available
689 (https://github.com/bendevlin18/human-fetal-RNASeq). Gene Ontology (GO) enrichment
690 analysis (Metascape[77]) was performed on genes with significant positive and negative
691 correlations separately ($p<0.05$).

692 All data is publicly available (GEO Accession number: GSE188872).

693 **Statistics**: Statistical tests, excluding RNA-sequencing analyses, were performed using
694 Graphpad Prism 9. Raw data as well as a description of the tests and results (including
695 multiple comparison corrections and post-hoc analyses) are provided. Unless otherwise
696 noted, data are mean ± s.e.m except for box plots (whiskers are min. to max., hinges of
697 boxes are 25th and 75th percentiles, middle line is the median). All analyses were
698 performed by an individual blind to animal sex, condition (maternal diet), and/or genotype.

In addition to correlation analyses in human tissues (see Fig 4e), we additionally ran a global ANCOVA to address the variance between the linear regressions by sex and tissue type. ANCOVA analysis confirms that the correlation between male fetal brain 5-HT levels and maternal triglyceride accumulation is significantly different than the correlations between male placental 5-HT levels and maternal triglyceride accumulation. It is also different than the correlations between female 5-HT levels and maternal triglyceride accumulation.

Acknowledgements: We thank the Duke University School of Medicine for the use of the Sequencing and Genomic Technologies Shared Resource, which provided library preparation and sequencing service. We also thank Kristina Sakers for guidance and R scripts for sequencing analysis.

Funding: Research reported in this publication was supported by the Eunice Kennedy Shriver National Institute of Child Health & Human Development (F32HD104430 to A.M.C.), the National Institute of Environmental Health Sciences (R01 ES025549 to S.D.B.), the Robert and Donna Landreth Family Foundation, and the Charles Lafitte Foundation.

Author Contributions: S.D.B, L.S., and J.B. conceived the study and, together with A.M.C, designed the experiments. A.M.C, B.A.D, J.B., L.A.G., YC.J, C.H., B.P., K.W., C.L.S., F.J., A.B.C-S, and E.R.L. performed experiments and data analysis. A.M.C. wrote the manuscript with contributions from all of the authors.

The authors declare no competing interests.

Supplementary Information is available for this paper.

Supplementary Table 1. Raw GO enrichment analysis results

Figure1-4_RawData_Stats. Raw data and detailed statistical information for Figures 1 through 4

Extended_Data_Fig1-9_RawData_Stats. Raw data and detailed statistical information for Extended Data Figures 1 through 9

Supplementary Table 2. PCR Primer sequences

*Correspondence and requests for materials should be addressed to Staci D. Bilbo (staci.bilbo@duke.edu)

743 1. Vickers, M. H., Breier, B. H., Cutfield, W. S., Hofman, P. L. & Gluckman, P. D. Fetal origins of
744 hyperphagia, obesity, and hypertension and postnatal amplification by hypercaloric nutrition. *Am J*
745 *Physiol Endocrinol Metab* **279**, E83-7 (2000).
746 2. Edlow, A. G. Maternal obesity and neurodevelopmental and psychiatric disorders in offspring. *Prenat*
747 *Diagn* **37**, 95–110 (2017).
748 3. Kott, J. & Brummelte, S. Trick or treat? Evaluating contributing factors and sex-differences for
749 developmental effects of maternal depression and its treatment. *Horm Behav* **111**, 31–45 (2019).
750 4. Krakowiak, P. *et al.* Maternal metabolic conditions and risk for autism and other neurodevelopmental
751 disorders. *Pediatrics* **129**, e1121-8 (2012).
752 5. Mina, T. H. *et al.* Prenatal exposure to very severe maternal obesity is associated with adverse
753 neuropsychiatric outcomes in children. *Psychological Medicine* **47**, 353–362 (2017).
754 6. Rivera, H., Christiansen, K. & Sullivan, E. The role of maternal obesity in the risk of neuropsychiatric
755 disorders. *Frontiers in Neuroscience* **9**, (2015).
756 7. Rodriguez, A. Maternal pre-pregnancy obesity and risk for inattention and negative emotionality in
757 children. *Journal of Child Psychology and Psychiatry* **51**, 134–143 (2010).
758 8. Robinson, M. *et al.* Pre-pregnancy maternal overweight and obesity increase the risk for affective
759 disorders in offspring. *Journal of Developmental Origins of Health and Disease* **4**, 42–48 (2013).
760 9. Deputy, N., Dub, B. & Sharma, A. J. Prevalence and Trends in Prepregnancy Normal Weight — 48
761 States, New York City, and District of Columbia, 2011–2015. *MMWR Morb Mortal Wkly Rep* **66**, 1402–
762 1407 (2019).
763 10. Hariri, N., Gougeon, R. & Thibault, L. A highly saturated fat-rich diet is more obesogenic than
764 diets with lower saturated fat content. *Nutr Res* **30**, 632–643 (2010).

765 11. Thompson, J. R. *et al.* Exposure to a High-Fat Diet during Early Development Programs Behavior
766 and Impairs the Central Serotonergic System in Juvenile Non-Human Primates. *Front Endocrinol*
767 *(Lausanne)* **8**, (2017).
768 12. Peleg-Raibstein, D., Luca, E. & Wolfrum, C. Maternal high-fat diet in mice programs emotional
769 behavior in adulthood. *Behavioural Brain Research* **233**, 398–404 (2012).
770 13. Bilbo, S. D. & Tsang, V. Enduring consequences of maternal obesity for brain inflammation and
771 behavior of offspring. *The FASEB Journal* **24**, 2104–2115 (2010).
772 14. Altemus, M., Sarvaiya, N. & Epperson, C. N. Sex differences in anxiety and depression clinical
773 perspectives. *Front Neuroendocrinol* **35**, 320–30 (2014).
774 15. McLean, C. P., Asnaani, A., Litz, B. T. & Hofmann, S. G. Gender Differences in Anxiety Disorders:
775 Prevalence, Course of Illness, Comorbidity and Burden of Illness. *J Psychiatr Res* **45**, 1027–35 (2011).
776 16. Cutler, G. J., Flood, A., Hannan, P. & Neumark-Sztainer, D. Major Patterns of Dietary Intake in
777 Adolescents and Their Stability over Time. *The Journal of Nutrition* **139**, 323–328 (2009).
778 17. Li, L. *et al.* Fast food consumption among young adolescents aged 12–15 years in 54 low- and
779 middle-income countries. *Glob Health Action* **13**, 1795438.
780 18. Fryar, C. D. & Ogden, C. L. Fast Food Intake Among Children and Adolescents in the United
781 States, 2015–2018. 8 (2020).
782 19. Cruz, F., Ramos, E., Lopes, C. & Araújo, J. Tracking of food and nutrient intake from adolescence
783 into early adulthood. *Nutrition* **55–56**, 84–90 (2018).
784 20. Hu, T. *et al.* Higher Diet Quality in Adolescence and Dietary Improvements Are Related to Less
785 Weight Gain During the Transition From Adolescence to Adulthood. *The Journal of Pediatrics* **178**, 188-
786 193.e3 (2016).

787 21. Scattoni, M. L., Crawley, J. & Ricceri, L. Ultrasonic vocalizations: a tool for behavioural
788 phenotyping of mouse models of neurodevelopmental disorders. *Neurosci Biobehav Rev* **33**, 508–515
789 (2009).
790 22. Yin, X. *et al.* Maternal Deprivation Influences Pup Ultrasonic Vocalizations of C57BL/6J Mice.
791 *PLoS One* **11**, (2016).
792 23. Van Segbroeck, M., Knoll, A. T., Levitt, P. & Narayanan, S. MUPET-Mouse Ultrasonic Profile
793 ExTraction: A Signal Processing Tool for Rapid and Unsupervised Analysis of Ultrasonic Vocalizations.
794 *Neuron* **94**, 465-485.e5 (2017).
795 24. Mun, H.-S., Lipina, T. V. & Roder, J. C. Ultrasonic Vocalizations in Mice During Exploratory
796 Behavior are Context-Dependent. *Frontiers in Behavioral Neuroscience* **9**, 316 (2015).
797 25. Mosienko, V., Beis, D., Alenina, N. & Wöhr, M. Reduced isolation-induced pup ultrasonic
798 communication in mouse pups lacking brain serotonin. in *Mol Autism* vol. 6 (2015).
799 26. Sachs, B. D., Ni, J. R. & Caron, M. Sex differences in response to chronic mild stress and
800 congenital serotonin deficiency. *Psychoneuroendocrinology* **40**, 123–9 (2014).
801 27. Angoa-Pérez, M. *et al.* Mice Genetically Depleted of Brain Serotonin Do Not Display a
802 Depression-like Behavioral Phenotype. *ACS Chem. Neurosci.* **5**, 908–919 (2014).
803 28. Savelieva, K. V. *et al.* Genetic Disruption of Both Tryptophan Hydroxylase Genes Dramatically
804 Reduces Serotonin and Affects Behavior in Models Sensitive to Antidepressants. *PLoS One* **3**, e3301
805 (2008).
806 29. Osipova, D. V., Kulikov, A. V. & Popova, N. K. C1473G polymorphism in mouse tph2 gene is
807 linked to tryptophan hydroxylase-2 activity in the brain, intermale aggression, and depressive-like
808 behavior in the forced swim test. *Journal of Neuroscience Research* **87**, 1168–1174 (2009).
809 30. Bonnin, A. *et al.* A transient placental source of serotonin for the fetal forebrain. *Nature* **472**,
810 347–350 (2011).

811 31. Song, L. *et al.* Prenatal high-fat diet alters placental morphology, nutrient transporter
812 expression, and mtorc1 signaling in rat. *Obesity (Silver Spring)* **25**, 909–919 (2017).
813 32. Goeden, N. *et al.* Maternal Inflammation Disrupts Fetal Neurodevelopment via Increased
814 Placental Output of Serotonin to the Fetal Brain. *J. Neurosci.* **36**, 6041–6049 (2016).
815 33. Edlow, A. G. *et al.* Placental Macrophages: A Window Into Fetal Microglial Function in Maternal
816 Obesity. *International Journal of Developmental Neuroscience* S0736574818302508 (2018)
817 doi:10.1016/j.ijdevneu.2018.11.004.
818 34. Roberts, K. A. *et al.* Placental structure and inflammation in pregnancies associated with obesity.
819 *Placenta* **32**, 247–54 (2011).
820 35. Etienne, F. *et al.* Two-photon Imaging of Microglial Processes' Attraction Toward ATP or
821 Serotonin in Acute Brain Slices. *JoVE (Journal of Visualized Experiments)* e58788 (2019)
822 doi:10.3791/58788.
823 36. Turkin, A., Tuchina, O. & Klempin, F. Microglia Function on Precursor Cells in the Adult
824 Hippocampus and Their Responsiveness to Serotonin Signaling. *Frontiers in Cell and Developmental*
825 *Biology* **9**, (2021).
826 37. Vetreno, R. P., Patel, Y., Patel, U., Walter, T. J. & Crews, F. T. Adolescent intermittent ethanol
827 reduces serotonin expression in the adult raphe nucleus and upregulates innate immune expression that
828 is prevented by exercise. *Brain, Behavior, and Immunity* **60**, 333–345 (2017).
829 38. Cunningham, C. L., Martinez-Cerdeno, V. & Noctor, S. C. Microglia regulate the number of neural
830 precursor cells in the developing cerebral cortex. *J Neurosci* **33**, 4216–33 (2013).
831 39. Block, C. L. *et al. Prenatal Environmental Stressors Impair Postnatal Microglia Function and Adult*
832 *Behavior in Males*. 2020.10.15.336669 https://www.biorxiv.org/content/10.1101/2020.10.15.336669v2
833 (2020) doi:10.1101/2020.10.15.336669.

834 40. Kopec, A. M., Smith, C. J., Ayre, N. R., Sweat, S. C. & Bilbo, S. D. Microglial dopamine receptor
835 elimination defines sex-specific nucleus accumbens development and social behavior in adolescent rats.
836 *Nature Communications* **9**, 1–16 (2018).
837 41. VanRyzin, J. W. *et al.* Microglial Phagocytosis of Newborn Cells Is Induced by Endocannabinoids
838 and Sculpts Sex Differences in Juvenile Rat Social Play. *Neuron* **102**, 435-449.e6 (2019).
839 42. Kolodziejczak, M. *et al.* Serotonin Modulates Developmental Microglia via 5-HT2B Receptors:
840 Potential Implication during Synaptic Refinement of Retinogeniculate Projections. *ACS Chem Neurosci* **6**,
841 1219–1230 (2015).
842 43. Krabbe, G. *et al.* Activation of serotonin receptors promotes microglial injury-induced motility
843 but attenuates phagocytic activity. *Brain Behav Immun* **26**, 419–28 (2012).
844 44. Béchade, C. *et al.* The serotonin 2B receptor is required in neonatal microglia to limit
845 neuroinflammation and sickness behavior in adulthood. *Glia* **69**, 638–654 (2021).
846 45. Baković, P. *et al.* Differential Serotonin Uptake Mechanisms at the Human Maternal–Fetal
847 Interface. *Int J Mol Sci* **22**, 7807 (2021).
848 46. Kliman, H. J. *et al.* Pathway of Maternal Serotonin to the Human Embryo and Fetus.
849 *Endocrinology* **159**, 1609–1629 (2018).
850 47. Medzhitov, R. Toll-like receptors and innate immunity. *Nat Rev Immunol* **1**, 135–145 (2001).
851 48. Reyna, S. M. *et al.* Elevated Toll-Like Receptor 4 Expression and Signaling in Muscle From Insulin-
852 Resistant Subjects. *Diabetes* **57**, 2595–2602 (2008).
853 49. Shi, H. *et al.* TLR4 links innate immunity and fatty acid–induced insulin resistance. *J Clin Invest*
854 **116**, 3015–3025 (2006).
855 50. Milanski, M. *et al.* Saturated Fatty Acids Produce an Inflammatory Response Predominantly
856 through the Activation of TLR4 Signaling in Hypothalamus: Implications for the Pathogenesis of Obesity.
857 *Journal of Neuroscience* **29**, 359–370 (2009).

858 51. Rivera, P. D. *et al.* Removal of microglial-specific MyD88 signaling alters dentate gyrus
859 doublecortin and enhances opioid addiction-like behaviors. *Brain Behav Immun* **76**, 104–115 (2019).
860 52. McAlees, J. W. *et al.* Distinct Tlr4-expressing cell compartments control neutrophilic and
861 eosinophilic airway inflammation. *Mucosal Immunol* **8**, 863–873 (2015).
862 53. Wang, Z. *et al.* Saturated fatty acids activate microglia via Toll-like receptor 4/NF-κB signalling.
863 *Br J Nutr* **107**, 229–241 (2012).
864 54. Li, M., Fu, W. & Li, X.-A. Differential fatty acid profile in adipose and non-adipose tissues in obese
865 mice. *Int J Clin Exp Med* **3**, 303–307 (2010).
866 55. Basu, S. *et al.* Pre-gravid obesity associates with increased maternal endotoxemia and metabolic
867 inflammation. *Obesity (Silver Spring)* **19**, 476–482 (2011).
868 56. Bowser, S. M. *et al.* Serum endotoxin, gut permeability and skeletal muscle metabolic
869 adaptations following a short term high fat diet in humans. *Metabolism* **103**, 154041 (2020).
870 57. Pendyala, S., Walker, J. M. & Holt, P. R. A High-Fat Diet Is Associated With Endotoxemia That
871 Originates From the Gut. *Gastroenterology* **142**, 1100-1101.e2 (2012).
872 58. Brown, A. G., Maubert, M. E., Anton, L., Heiser, L. M. & Elovitz, M. A. The tracking of
873 lipopolysaccharide through the feto-maternal compartment and the involvement of maternal TLR4 in
874 inflammation-induced fetal brain injury. *American Journal of Reproductive Immunology* **82**, e13189
875 (2019).
876 59. Hirschmugl, B. *et al.* Maternal obesity modulates intracellular lipid turnover in the human term
877 placenta. *Int J Obes* **41**, 317–323 (2017).
878 60. Saben, J. *et al.* Maternal obesity is associated with a lipotoxic placental environment. *Placenta*
879 **35**, 171–177 (2014).
880 61. Calabuig-Navarro, V. *et al.* Effect of Maternal Obesity on Placental Lipid Metabolism.
881 *Endocrinology* **158**, 2543–2555 (2017).

882 62. Qiao, L. *et al.* Maternal High-Fat Feeding Increases Placental Lipoprotein Lipase Activity by
883 Reducing SIRT1 Expression in Mice. *Diabetes* **64**, 3111–3120 (2015).
884 63. Liu, Y. *et al.* Single-cell RNA-seq reveals the diversity of trophoblast subtypes and patterns of
885 differentiation in the human placenta. *Cell Res* **28**, 819–832 (2018).
886 64. Wadsack, C., Desoye, G. & Hiden, U. The feto-placental endothelium in pregnancy pathologies.
887 *Wien Med Wochenschr* **162**, 220–224 (2012).
888 65. VanWijk, M. J., Kublickiene, K., Boer, K. & VanBavel, E. Vascular function in preeclampsia.
889 *Cardiovascular Research* **47**, 38–48 (2000).
890 66. Sternberg, E. M., Trial, J. & Parker, C. W. Effect of serotonin on murine macrophages:
891 suppression of Ia expression by serotonin and its reversal by 5-HT2 serotonergic receptor antagonists. *J*
892 *Immunol* **137**, 276–282 (1986).
893 67. Sternberg, E. M., Wedner, H. J., Leung, M. K. & Parker, C. W. Effect of serotonin (5-HT) and other
894 monoamines on murine macrophages: modulation of interferon-gamma induced phagocytosis. *J*
895 *Immunol* **138**, 4360–4365 (1987).
896 68. Bordt, E. A., Block, C. L. ,. Petrozziello, T. ,. Sadri-Vakili, G. ,. Smith, C. J. ,. Edlow, A. G. ,. Bilbo, S.
897 D. Isolation of Microglia from Mouse or Human Tissue. *STAR Protocols* (2020)
898 doi:10.1016/j.xpro.2020.100035.
899 69. Sánchez, C. L., Van Swearingen, A. E. D., Arrant, A. E., Kuhn, C. M. & Zepf, F. D. Dietary
900 manipulation of serotonergic and dopaminergic function in C57BL/6J mice with amino acid depletion
901 mixtures. *J Neural Transm (Vienna)* **121**, 153–162 (2014).
902 70. Quinlan, C. & Peters, C. Endotoxin detection using a colorimetric, kinetic microplate reader assay
903 and integrated data analysis. 2.
904 71. Cox, K. H. & Rissman, E. F. Sex differences in juvenile mouse social behavior are influenced by
905 sex chromosomes and social context. *Genes Brain Behav* **10**, 465–472 (2011).

906 72. An, X.-L. *et al.* Strain and sex differences in anxiety-like and social behaviors in C57BL/6J and
907 BALB/cJ mice. *Exp Anim* **60**, 111–123 (2011).
908 73. Seibenhener, M. L. & Wooten, M. C. Use of the Open Field Maze to Measure Locomotor and
909 Anxiety-like Behavior in Mice. in *J Vis Exp* (2015). doi:10.3791/52434.
910 74. Moy, S. S. *et al.* Sociability and preference for social novelty in five inbred strains: an approach
911 to assess autistic-like behavior in mice. *Genes, Brain and Behavior* **3**, 287–302 (2004).
912 75. Langmead, B. Aligning short sequencing reads with Bowtie. *Current protocols in bioinformatics /*
913 *editoral board, Andreas D. Baxevanis ... [et al.]* **CHAPTER**, Unit (2010).
914 76. Robinson, M. D., McCarthy, D. J. & Smyth, G. K. edgeR: a Bioconductor package for differential
915 expression analysis of digital gene expression data. *Bioinformatics* **26**, 139–140 (2010).
916 77. Zhou, Y. *et al.* Metascape provides a biologist-oriented resource for the analysis of systems-level
917 datasets. *Nat Commun* **10**, 1523 (2019).
918